CH/Tech/95/02

Hybrid Tests

Report on beam tests at the ANU

Author: Steven Singer

Date: 1 July 1995

Gas Hybrid Detector Tests

1 Introduction

A series of experiments have been performed to explore the behaviour of the gas cell in the CHARISSA gas-silicon hybrid detectors [1]. The hybrids comprise a 50 mm deep longitudinal ΔE section and a 50×50 mm^2 Si strip detector with 16 strips (each 3 mm wide) orientated parallel to the reaction plane. A cross-section of a detector is shown in figure 1. The experiments were performed with a view to finding ways of improving the performance of the detectors.

The effects of all operating parameters have been quantitatively studied and recommendations made for their optimal values. A position dependence of the ΔE system has been identified. Its dependence of different particle types and grid configurations has been measured.

2 Experiment and analysis description

The experiments involved a series of beams elastically scattered from a gold target. Elastic scattering was chosen to reduce the energy spread of particles entering the detector and the scattered energy was essentially constant over the whole detector surface.

A systematic variation of operating parameters used an ^{16}O beam at 31.1, 48.6 and 70 MeV to study the effect they had on resolution and efficiency. Other runs analysed involved a ^{12}C beam at 45 MeV (April 1994), and a ^{40}Ca beam at 190 MeV (September 1993). Data taken by Neil Curtis [1,2] for the scattering of ^{12}C at 84 MeV (September 1993) were also analysed for comparison.

Known problems with the design were :

- The grid wires shadowed the detector, reducing its efficiency by 10% per grid

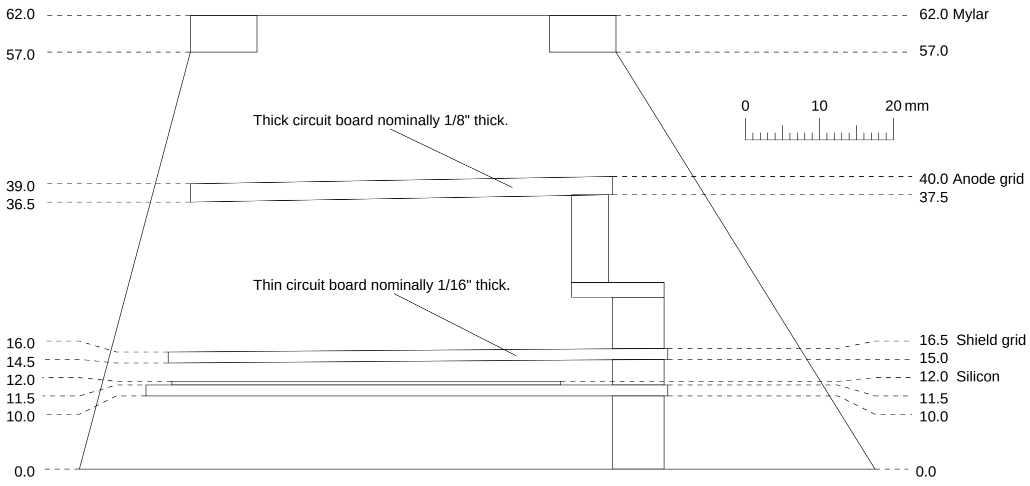

Figure 1: Cross-section of the interior of a detector. All measurements are in mm unless otherwise stated.

plane. This gave an overall reduction of 19% for a single detector. With 2 detectors used in coincidence, the overall reduction was 34%.

- The ΔE signal appeared to vary with position across the detector.
- The grid wire shadowing led to dips in angular distribution measurements (particularly in singles data) since the grid wires were orientated parallel to the reaction plane.

Alterations tried were :

- Using thinner grid wires.
- Removing the shield grid.
- Using a metalised PET sheet instead of a grid.
- Altering grid wire orientation to be parallel to the strips.
- Altering the operating bias.
- Altering the amplifier shaping time.

In the main experiment, three sets of runs were performed using different grid configurations. The configurations are summarised in table 1. For each configuration, three beam energies were used, namely 31.1, 48.6 and 70 MeV. Shaping times of 1, 2 and 3 μs and bias voltages of 190, 380, 570 and 760 V corresponding 1, 2, 3 and 4 V cm^{-1} τ^{-1} were employed. 760 V measurements were only performed for run set 2 since this was at the verge of electrical breakdown, and the preamplifier

Set	Detector	Anode grid		Shield grid	
		Wire Thickness	Orientation	Wire Thickness	Orientation
1	1	100 μm	Horizontal	100 μm	Vertical
	3	100 μm	Vertical	20 μm	Horizontal
2	1	1 μm PET	—	blank	—
	3	20 μm	Vertical	20 μm	Vertical
3	1	20 μm	Horizontal	blank	—
	3	20 μm	Vertical	blank	—

Table 1: Combinations of grids used in detector tests.

was placed at risk. At 48.6 MeV all bias voltage and shaping time combinations were tried and the optimum values inferred. For the other beam energies the two parameters were varied individually with the other held at its inferred optimum.

3 Analysis

For the off-line analysis, the program divided the detector into pixels. The pixel size was 3 mm in the Y direction (determined by the silicon strip width) and 0.75 mm in the X direction (giving 64 × 16 pixels).

For particles incident in each pixel of the silicon detector, the corresponding ΔE signals were averaged, and the width (standard deviation) of the peak was extracted. In this procedure, small signals attributable to noise were discarded. The range of channels defining the peak was determined by inspection of the sum spectrum of all the pixels and then the individual pixels were automatically analysed within this window.

For cases when the X-Y position dependence was not being specifically studied, the analysis selected a range of pixels at the centre of the detector acceptance. For analysis of signal heights, this area was 4 × 1 pixels (3 × 3 mm^2), for analysis of signal widths the area was 20 × 5 pixels (15 × 15 mm^2). A small area was used for the signal height averaging to reduce the effect of the systematic variation of the ΔE signal with position. A larger area was used for the width as the width was roughly constant with detector position so an averaging could be performed on many points to reduce statistical effects. The error in the width was estimated, as in the case of the ΔE itself, by calculating the standard deviation of the individual pixel measurements and dividing by the square root of the number of pixels.

4 Effect of the diameters of the grid wires

The two grid planes in the detectors served different purposes and could have placed different requirements on the wire diameters. The best choice for the shield grid was complicated because it might have operated as either an electrostatic shield plane or as a physical barrier to positive ions reaching the silicon detector.

The two main unwanted effects of the grid wires were their reduction of efficiency, and their effect on angular distributions. Four main ways of overcoming the reduction of efficiency and the shadowing were tried :

- Using thinner grid wires. Going from 100 μm wires to 20 μm wires would reduce the effect per grid plane from 10% to 2%. This would reduce, but not eliminate, the shadowing.
- Removing the shield grid. This would halve the efficiency loss in the detector, and also halve the number of shadows.
- Using an metalised PET sheet instead of wires. This would remove the shadowing entirely, but at a possible cost to resolution due to straggling in the PET sheet.
- Altering the wire orientation to be horizontal (parallel to the strips). This would have no effect on the efficiency, but since the strips were 3 mm wide, any shadowing should be undetectable.

Each of these changes had the anticipated effect on the shadowing, and presumably on the efficiency. The shadowing from the 20 μm wires when orientated vertically was barely detectable, but still at a level that affects angular distribution measurements. Dips in the position spectrum were observed to be approximately 7% for the whole, gain-matched detector. With horizontal wires or the PET anode no shadowing was seen.

5 Linearity

The measured signal height was plotted against the predicted energy loss calculated with *dedx* and found to show excellent linearity (see figure 2).

The offsets for the two telescopes were 60.0 and 42.2 channels respectively. These correspond to 0.98 and 0.58 MeV. The offsets were attributed to either offsets in the ADCs, or base line effects in the amplifiers.

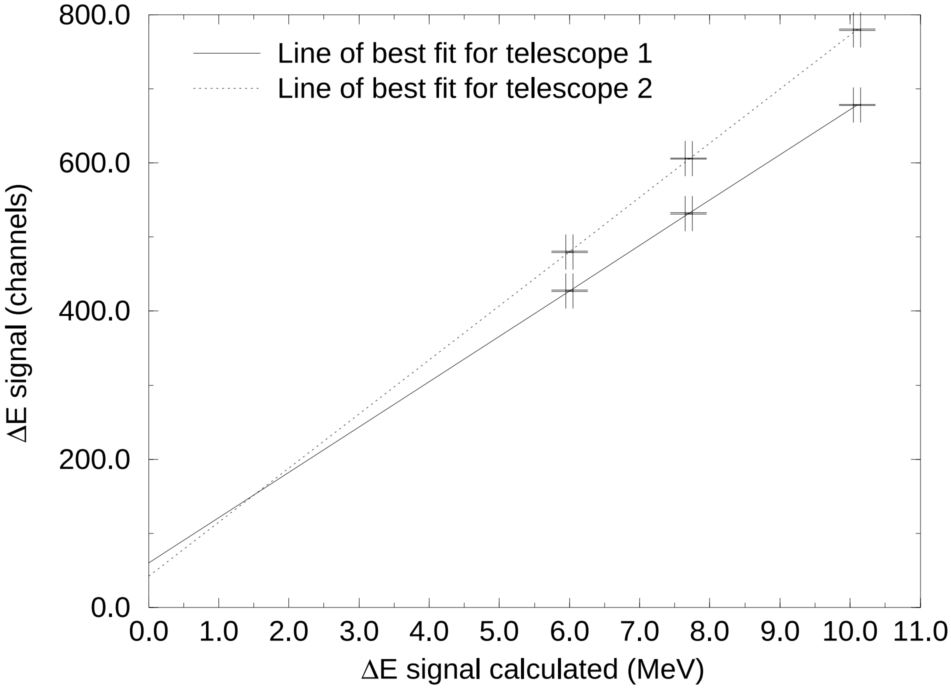

Figure 2: Comparison of predicted and measured ΔE loss for run set 3.

6 Shaping time and bias voltage effects

The effects of the shaping time and bias voltage on the height and resolution of the ΔE signal were investigated. Only the central portion of the detector was used for this analysis. Since the calibration of the spectrum was dependent on the operating parameters, the peak widths obtained in the analysis were expressed as a percentage of the signal height. Note that this quantity is, apart from a constant factor, the resolution in keV. Sample results are shown in figure 3.

It was found that the signal height at 1 μs tended to be lower than at the other shaping times. Under these circumstances the peak width (measured as a percentage of signal height) also increased, but by more than would be expected simply from the reduction in height. That is, the width measured in channels got worse.

Similarly a bias of 1 V cm^{-1} τ^{-1} performed poorly compared to the other biases. The tendency towards degraded resolution was particularly evident for 1 μs and 1 V cm^{-1} τ^{-1}used together.

It is deduced that, particularly at 1 V cm^{-1} τ^{-1}, the charge collection time for the signal was becoming comparable to 1 μs. This meant that not all the charge was being collected, directly giving the reduction in signal height. The increase in peak width is also explained if not all the charge was collected as statistical fluctuations

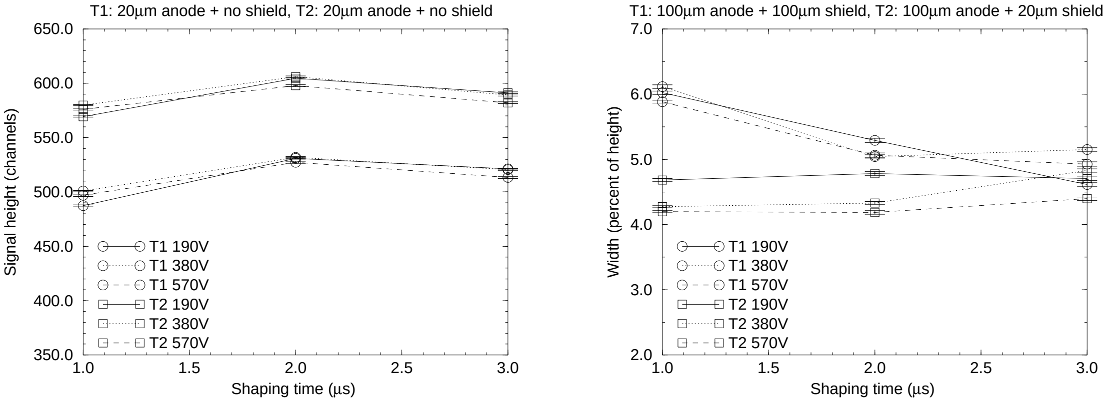

Figure 3a: Signal height variation. Figure 3b: Signal width variation.

Figure 3: Variation of signal height (a) and width (b) with shaping time and bias voltage. The values for the width in the figure are standard deviations.

would be relatively more important.

The resolution performance does not distinguish between 2 and 3 μs, or between 2, 3 and 4 V cm^{-1} τ^{-1}. However, the higher biases are fraught with other dangers. During one run (in run set 2) at 4 V cm^{-1} τ^{-1}, a preamplifier was damaged by electrical breakdown and had to be replaced. On a separate experiment, running at approximately 3 V cm^{-1} τ^{-1}, the ΔE detector was seen to fire continuously until its bias was reduced. This was attributed to micro-discharges. With regard to shaping times, the choice of a 3 μs shaping time, was rejected as there is a larger probability of pileup than at 2 μs.

It may be noted that when the preamplifier was replaced in the experiment, as mentioned above, the signal height was seen to increase and the relative signal width decrease by the same factor. This meant that the width in volts stayed constant when the preamplifier was replaced.

The recommended operating parameters are the lowest bias voltage and shaping time that give no reduction in the performance. On the basis of the recent observations, these are 2 μs shaping time and 2 V cm^{-1} τ^{-1} bias.

7 Position variation

The variation of the ΔE signal with position was investigated. The effect of bias voltage, shaping time and grid configuration was analysed. The signal height was measured as a function of detector position and these measurements were used to build up a 3 dimensional surface showing the variation of signal height with position. This surface had a characteristic “armchair” shape with ridges at 3 edges of the detector, and a sharp fall-off towards the side of the detector where

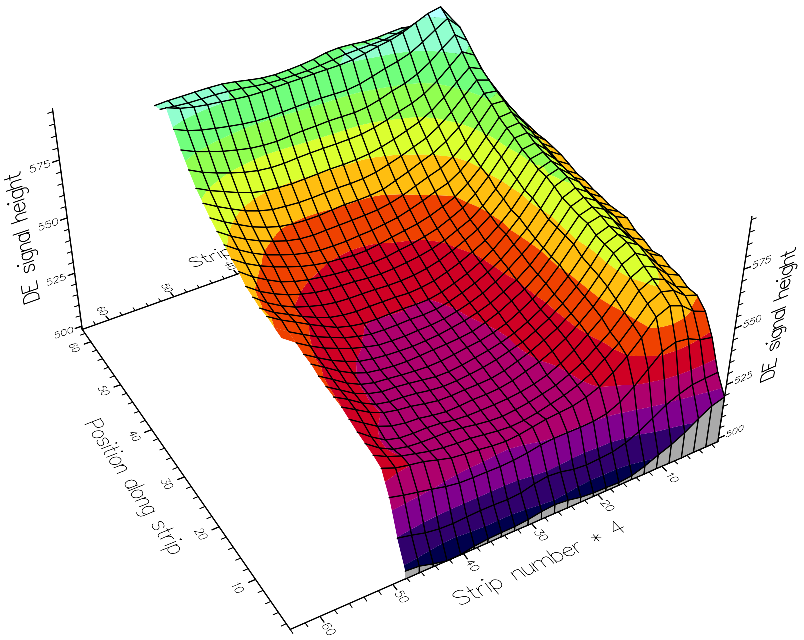
DE signal height
500
525
550
575
Strip
60
50
40
Position along strip
60
50
40
30
20
10
Strip number * 4
60
50
40
30
20
10
DE signal height
500
525
550
575